Grafting of Vapor-Grown Carbon Nanofibers via in-Situ Polycondensation of 3-Phenoxybenzoic Acid in Poly(phosphoric acid)

Jong-Beom Baek,*,†,‡ Christopher B. Lyons,§ and Loon-Seng Tan*,⊥

School of Chemical Engineering, Chungbuk National University, Cheongju, Chungbuk, 361-763 South Korea; University of Dayton Research Institute, 300 College Park, Dayton, Ohio 45469-0168; Southwestern Ohio Council for Higher Education, 3155 Research Blvd., Suite 204, Dayton, Ohio 45420-4015; and Polymer Branch, Materials & Manufacturing Directorate, AFRL/MLBP, Air Force Research Laboratory, Wright-Patterson Air Force Base, Dayton, Ohio 45433-7750

Received May 25, 2004; Revised Manuscript Received August 14, 2004

ABSTRACT: In-situ polymerization of 3-phenoxybenzoic acid in the presence of various amounts (1−30 wt %) of vapor-grown carbon nanofibers (VGCNF) was carried out in poly(phosphoric acid)/phosphorus pentoxide (PPA/P_2O_5; 1:4 w/w) medium. 3-Phenoxybenzoic acid polymerizes via Friedel−Crafts acylation in PPA to form poly(oxy-1,3-phenylenecarbonyl-1,4-phenylene) or *m*PEK. The resulting *m*PEK-*g*-VGCNF products that contained less than 10 wt % of VGCNF were soluble in *N*-methyl-2-pyrrolidinone and had intrinsic viscosity values ranging from 1 to 1.73 dL/g in methanesulfonic acid (MSA) at 30 ± 0.1 °C. The overall evidence based on the data from elemental analysis (EA), thermogravimetric analysis (TGA), and Fourier transform infrared spectroscopy (FT-IR) as well as scanning electron and transmission electron microscopies of the resulting materials implicates that VGCNF remained more or less structurally intact under the mildly acidic, relatively high-shearing and hot polymerization conditions. It is also evident that under these reaction conditions *m*PEK was grafted onto the surface of VGCNF, resulting in the formation of "hairy tubes". The wide-angle X-ray diffraction result showed the growth of the 3.35 Å peak characteristic of VGCNF that increased in intensity proportionately to the presence of VGCNF in the sample and correlated well with the EA and TGA results. The conductivity of the cast film (10 wt % VGCNF) is 0.25 S/cm (bottom of film) and 0.30 S/cm (top of film).

Introduction

In comparison to single-walled (SWNT) or multi-walled carbon nanotubes (MWNT), vapor-grown carbon nanofibers (VGCNF) are more attractive from the standpoint of practicality in terms of their relatively low cost and availability in larger quantities as the result of their more advanced stage in commercial production. These nanofibers are typically produced by a vapor-phase catalytic process in which a carbon-containing feedstock (e.g., CH_4, C_2H_4, etc.) is pyrolyzed in the presence of small metal catalyst (e.g., ferrocene, $Fe(CO)_5$, etc.). They have an outer diameter of 60−200 nm, a hollow core of 30−90 nm, and length on the order of 50−100 μm.[1−3] It follows that having aspect ratios (length/diameter) of greater than 800 should make them useful as nanolevel reinforcement for polymeric matrices. Furthermore, since their inherent electrical and thermal transport properties are also excellent, there are many possibilities imaginable for tailoring their polymer matrix composites into affordable, lightweight, multifunctional materials.

Conceptually, there are three general techniques for dispersing chemically unmodified VGCNF in the polymer matrices: (1) melt blending, (2) solution blending, and (3) reaction blending. For the reaction blending route, there are two scenarios: (a) in-situ polymerization of monomers (AB) or comonomers (AA + BB) in the presence of dispersed VGCNF that occurs without forming any covalent bonding between the VGCNF and the matrix polymer or (b) in-situ grafting of AB monomers that occurs with direct covalent bonds formed between the VGCNF and the matrix polymer. While melt-blending is perhaps the most cost-effective approach to VGCNF-based nanocomposites, and has been applied to thermoplastic,[1,4] thermosetting,[5] and elastomeric[6] matrices, the resulting nanocomposite materials are by and large less than optimal. This is especially true in the cases where polymer−VGCNF incompatibility adversely impacts the desired level of dispersion and the breakage of the carbon nanofibers by high shear forces reduces the reinforcing aspect ratios.[7] The solution blending appears to have circumvented these problems; for example, the nanocomposite materials produced by this route have shown 2−3 orders of magnitude higher in electrical conductivity and much lower percolation threshold (<1 vol %) than similar materials prepared by the melt-blending route.[8] To our knowledge, we are not aware of any report in the literature that describes successful preparation of VGCNF-based nanocomposite materials via reaction blending.[9] However, similar nongrafting, reaction blending processes have been reported for unmodified SWNT[10] and MWNT.[7,11−15] In addition, there are reports on the grafting of a polymer either to or from a SWNT or MWNT that typically involved prior oxidation[16,17] or functionalization of the CNT with a reactive group (e.g., surface-bound acid chloride[18] or initiator for atom-transfer radical polymerization[19]).

In this paper, we extend our work on functionalization of VGCNF via a direct Friedel−Crafts arylcarbonylation in poly(phosphoric acid)[20] to in-situ polymerization of an AB monomer for a *meta*-poly(ether−ketone) or *m*PEK. In addition, the results of our approach also

† Chungbuk National University.
‡ University of Dayton Research Institute.
§ Southwestern Ohio Council for Higher Education.
⊥ Wright-Patterson Air Force Base.
* Corresponding authors. E-mail loon-seng.tan@wpafb.af.mil or jbbaek@chungbuk.ac.kr.

10.1021/ma048964o CCC: $27.50
Published on Web 09/30/2004

implicate the covalent attachment (grafting) of *m*PEK to the VGCNF.

Experimental Section

Materials. All reagents and solvents were purchased from Aldrich Chemical Inc. and used as received, unless otherwise specified. The commercially available AB monomer, 3-phenoxybenzoic acid (Aldrich Chemical Co.), was recrystallized from heptane to give white needles (mp 146−147 °C). Vapor-grown multiwalled carbon nanofiber (VGCNF, PR-19-HT) was obtained from Applied Science Inc., Cedarville, OH.[1,21]

Instrumentation. Infrared (FT-IR) spectra were recorded on a Thermo Nicolet Fourier transform spectrophotometer. Raman spectra were taken using a Thermo Nicolet Almega dispersion visible Raman spectrometer. Elemental analysis and mass spectral analysis were performed by the System Supports Branch, Air Force Research Lab, Dayton, OH. The melting points (mp) of all the compounds were determined on a Mel-Temp melting point apparatus and are uncorrected. Intrinsic viscosities were determined with Cannon-Ubbelohde No. 150 viscometers. Flow times were recorded for methanesulfonic acid (MSA) solution and polymer solutions with concentrations of approximately 0.5−0.10 g/dL at 30.0 ± 0.1 °C. Differential scanning calorimetry (DSC) was performed under a nitrogen atmosphere with heating and cooling rates of 10 °C/min using a Perkin-Elmer DSC-7. The T_g's were taken from maximum inflections in baseline on DSC thermograms. Thermomechanical analysis (TMA) was conducted in helium with a heating rate of 4 °C/min using a TA Instrument model TMA 2940. The samples were compression-molded at 260−300 °C. The T_gs were taken from maximum inflections in baseline on TMA thermograms. Thermogravimetric analysis (TGA) was conducted in helium and air atmospheres with a heating rate of 10 °C/min using a TA Hi-Res TGA 2950 thermogravimetric analyzer. The transmission electron microscope (TEM) employed in this work was a Philips CM-200 TEM with a LaB6 filament operating at 200 kV. For TEM, samples were embedded in epoxy and 50−70 nm thick sections were microtomed at room temperature using a Reichert-Jung Ultracut Microtome. The samples were mounted on 200 mesh copper grids. The scanning electron microscope (SEM) used in this work was a Hitachi S-5200. Wide-angle X-ray diffractions (WAXS) of compression-molded samples were recorded with a Rigaku RU-200 diffractometer using Ni-filtered Cu Kα radiation (40 kV, 100 mA, $\lambda = 0.154$ 18 nm).

Representative Procedure for in-Situ Polymerization (*m*PEK with 10 wt % VGCNF Load). Into a 250 mL resin flask equipped with a high-torque mechanical stirrer, nitrogen inlet and outlet, and an solid-addition port, 3-phenoxybenzoic acid (2.7 g, 12.6 mmol), VGCNF (0.3 g), and PPA (83% P_2O_5 assay; 60 g) were placed and stirred under dry nitrogen purge at 130 °C for 3 h. P_2O_5 (15.0 g) was then added in one portion. The initially dark mixture (due to dispersion of VGCNF) became lighter and more viscous as the functionalization of VGCNF progressed. After 1 h at 130 °C, the reaction mixture was so viscous that it started to stick to the stirring rod. The temperature was maintained at 130 °C for 48 h. At the end of the reaction, the color of mixture was dark brown, and water was added into the flask. The resulting purple polymer clusters were put into a Waring blender, and the polymer bundles were chopped, collected by suction filtration, and washed with diluted ammonium hydroxide. An attempt was made to conduct a Soxhlet extraction on the polymeric product with methylene chloride, but it was aborted after a few hours because the glass thimble (filter) was clogged by the swollen polymeric product. No starting monomer was detected in the CH_2Cl_2 extract. Thus, the polymeric product was then Soxhlet-extracted with water for 3 days and then with methanol for 3 more days and was finally dried over phosphorus pentoxide under reduced pressure (0.05 mmHg) at 140 °C for 72 h to give the product in quantitative yield. Anal. Calcd for $C_{14.98}H_8O_2$: C, 81.78%; H, 3.67%; O, 14.54%. Found: C, 81.40%; H, 3.61%; O, 13.16%. FT-IR (KBr; cm^{-1}): 607, 711, 757, 847, 878, 971, 1013, 1159, 1239, 1271, 1307, 1434, 1480, 1501, 1576, 1594, 1658, 3065, 3438.

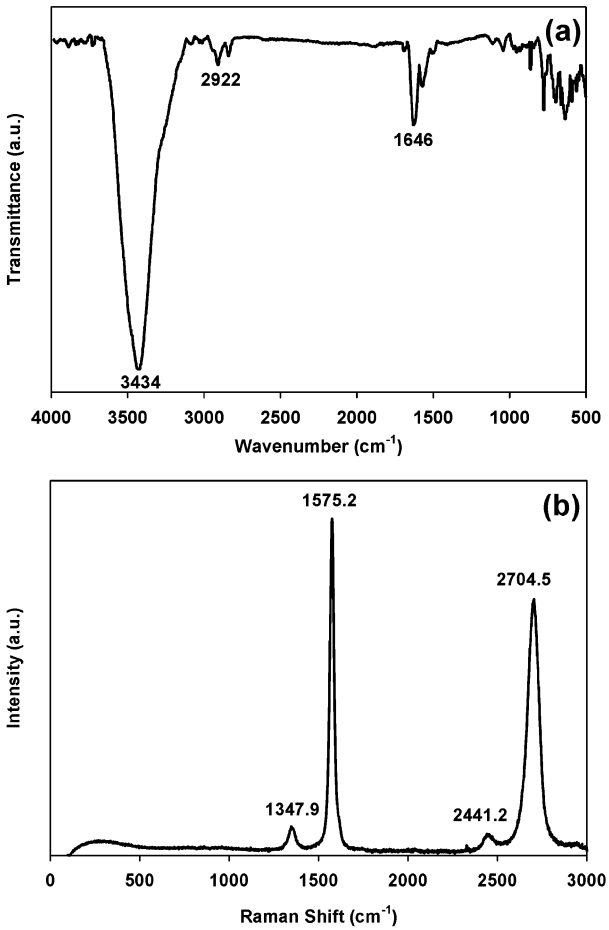

Figure 1. (a) FT-IR (KBr pellet) spectrum of VGCNF. (b) Raman spectrum of VGCNF.

Table 1. Elemental Analysis Data for VGCNF

sample	elemental analysis	C (%)	H (%)	O (%)
VGCNF	calcd	100.00	0.00	0.00
	found	98.87	1.10	<0.20[a]

[a] Below detection limit.

Results and Discussion

Characterization of VGCNF. The diameter and length of the VGCNF (Pyrograf III-19-HHT) used in this work were in the ranges 100−200 nm and 30−100 μm, respectively. These VGCNF were heat-treated up to 3000 °C to graphitize the surface carbon and remove residual iron catalyst and to improve the associated conducting properties. Since these vapor-grown carbon nanofibers (as opposed to carbon nanofibers from electrospinning process[22]) have hollow and concentric cores,[23] some researchers have considered them as MWNTs.[24,25]

For the purpose of having a basic understanding of the starting material, the as-received VGCNF was characterized by elemental analysis (Table 1), FT-IR spectroscopy (Figure 1a), Raman spectroscopy (Figure 1b), and TGA (Figure 5). It is noteworthy that the as-received VGCNF contains a significant amount of hydrogen (1.10 wt %), presumably attributable to the sp^3 C−H and sp^2 C−H defects as methane is used as the major component in the feedstock for its production.[1] This is consistent with the fact that carbon nanotubes

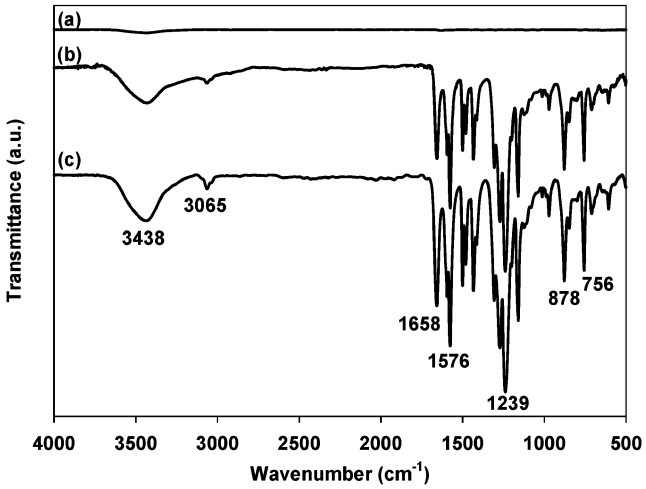

Figure 2. FT-IR spectra: (a) VGCNF, (b) 10 wt % *m*PEK-*g*-VGCNF, (c) *m*PEK.

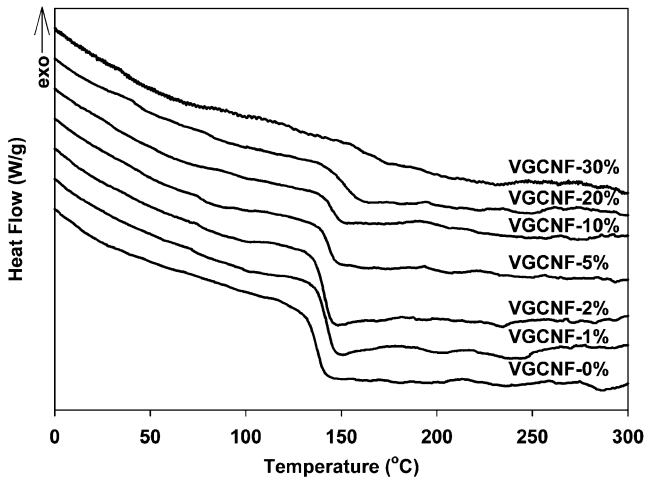

Figure 3. DSC thermograms of *m*PEK-*g*-VGCNF samples run with a heating rate of 10 °C/min.

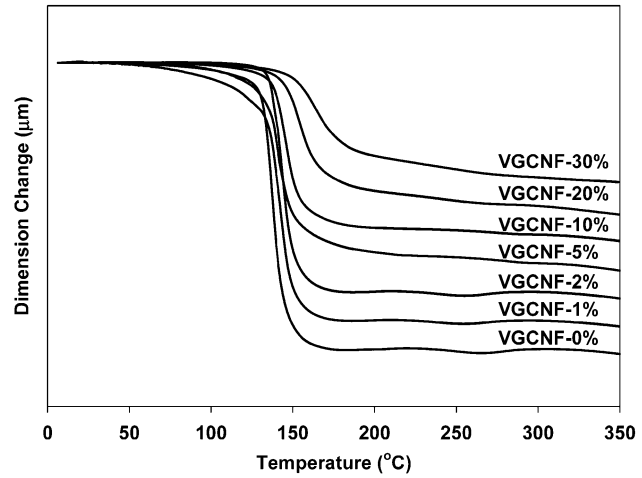

Figure 4. TMA thermograms of *m*PEK-*g*-VGCNF samples run with a heating rate of 4 °C/min.

or nanofibers grown from chemical vapor processes (CVD) possess more defects on the surface in comparison with MWNTs from the arc-discharge method. Accordingly, the datum seems to suggest an upper limit that for every eight carbon atoms there is a hydrogen atom attached.

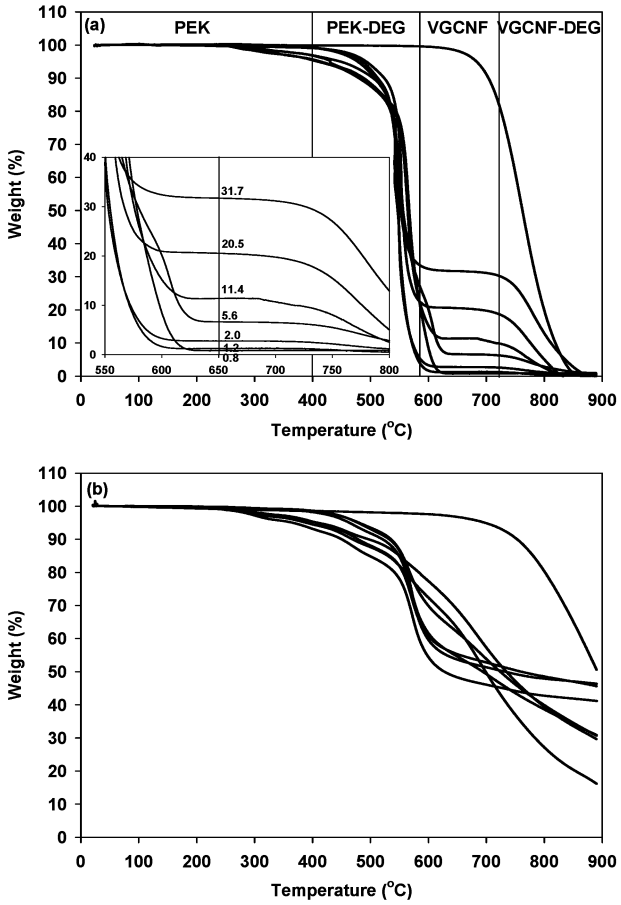

Figure 5. TGA thermograms of *m*PEK-*g*-VGCNF samples: (a) in air; the inset shows the residues due to VGCNF in wt % at 650 °C; (b) in helium.

Additionally, the FT-IR spectrum of as-received VGCNF exhibited small sp^2 C−H and sp^3 C−H stretching bands around 2922 cm^{-1} (Figure 1a) that are attributable to the defects at sidewalls and open ends of VGCNF. Logically, these defects would provide sites susceptible to the electrophilic substitution reaction. The large IR band observed at 3434 cm^{-1} and the weak bands around 1646 cm^{-1} are ascribable to the asymmetrical stretching and scissoring vibrations, respectively, stemming from the trace of water in the KBr pellet. The trace of water could not be removed even with extensive drying of the KBr at elevated temperatures prior to sample preparation and prolonged purging of the instrument with a stream of nitrogen gas.

The Raman spectrum for the as-received VGCNF is depicted in Figure 1b. The general sharpness of the bands and narrowness of the bandwidths are indicative of relatively high structural order as the consequence of high heat treatment.[26] As expected, there are no radial breathing modes (RBM) in the range 180−260 cm^{-1}, which are unique for single-wall carbon nanotubes.[27−30] In addition, VGCNF displayed a strong graphite mode or G band at 1575 cm^{-1} and a much weaker defect-induced Raman band (defect mode or D band) at 1348 cm^{-1}.[26] Since a similar band at ca. 1290 cm^{-1} observed for SWNT was thought to possibly be the sp^3-hybridized carbons in the nanotube walls,[27a,b] we tentatively attribute the peak at 1348 cm^{-1} to the sp^3-hybridized carbon atoms that are probably located at open end of VGCNF. Finally, in the region 2000−3000 cm^{-1} where the second-order G' band ∼2680 cm^{-1} for

Scheme 1. In-Situ Polymerization of 3-Phenoxybenzoic Acid with VGCNF: (a) PPA/P_2O_5, 130 °C

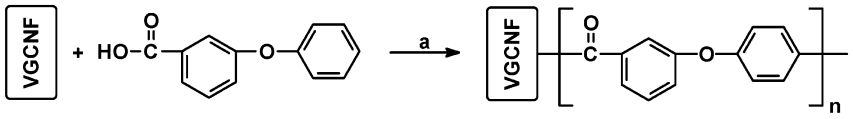

Table 2. Experimental VGCNF:AB Monomer Weight Ratios, Calculated and TGA-Determined VGCNF:*m*PEK Compositions, Intrinsic Viscosity, and Elemental Analysis Data for *m*PEK-*g*-VGCNF

feed		calculated[a]		found[b]		elemental analysis			
VGCNF (wt %)	PBA (wt %)	VGCNF (wt %)	*m*PEK (wt %)	VGCNF (wt %)	$[\eta]$[c] (dL/g)		C (%)	H (%)	O (%)
30	70	31.9	68.1	31.7		calcd[d]	86.08	2.81	11.11
						found	84.14	3.21	9.79
20	80	21.4	78.6	20.5		calcd[d]	83.95	3.23	12.81
						found	83.64	3.19	11.88
10	90	10.8	89.2	11.4		calcd[d]	81.78	3.67	14.54
						found	81.40	3.61	13.16
5	95	5.4	94.6	5.6	1.73	calcd[d]	80.68	3.89	15.42
						found	80.21	4.19	14.48
2	98	2.2	97.8	2.0	1.00	calcd[d]	80.02	4.03	15.95
						found	80.06	4.17	15.07
1	99	1.1	98.9	1.2	1.42	calcd[d]	79.80	4.07	16.13
						found	79.91	4.25	15.11

[a] Calculation based on the assumption that VGCNF is 100% C and the molar mass of the repeat unit of *m*PEK ($C_{13}H_8O_2$) is 196.20. [b] Residual weight percent at 650 °C from TGA thermograms in helium. [c] Intrinsic viscosity measured in MSA at 30.0 ± 0.1 °C. [d] Empirical formulas derived from the molar ratios of VGCNF:*m*PEK, i.e., C: $C_{13}H_8O_2$ are as follows: (30/70) $C_{20.64}H_8O_2$; (20/80) $C_{17.46}H_8O_2$; (10/90) $C_{14.98}H_8O_2$; (5/95) $C_{13.94}H_8O_2$; (2/98) $C_{13.96}H_8O_2$; (1/99) $C_{13.18}H_8O_2$.

SWNT appears,[31] we observed a strong, slightly broader band at 2705 cm^{-1} and a weaker band at 2441 cm^{-1}. While we are uncertain about the true origins of these bands, we suspect that their existence may be caused by the defect sites. Nevertheless, the collective evidence of elemental analysis, FT-IR, and Raman spectroscopic results seemed to suggest that VGCNF could provide reactive sites such as sp^2 C−H and sp^3 C−H for the electrophilic substitution reaction.

On the basis of the foregoing rationalization, we have recently reported for the first time that Friedel−Crafts acylation in poly(phosphoric acid) (PPA) is a viable, alternative route to effecting a controlled functionalization of VGCNF.[20] We accomplished this with 2,4,6-trimethylphenoxybenzoic acid in PPA using the improved conditions that we previously described.[32] The progress of the reaction was conveniently monitored with FT-IR spectroscopy following the temporal growth of the keto-carbonyl band at 1664 cm^{-1} associated with the product. In addition to scanning electron microscopic and UV−vis spectroscopic data, the combined results from the elemental analysis and thermogravimetric analysis further suggested that there were 3 arylcarbonyl groups covalently attached to the nanotube structure for every 100 carbon sites. Because of the presence of significant hydrogen content in the starting VGCNF, we concluded that the covalent attachment of the arylcarbonyl groups most probably occurred at the sp^2 C−H sites.

In-Situ Polycondensation. We have selected poly(oxy-1,3-phenylenecarbonyl-1,4-phenylene) or *m*PEK as the polymer matrix mainly because (a) the AB monomer, 3-phenoxybenzoic acid (PBA), is available commercially and (b) high-MW *m*PEK can be synthesized from PBA in PPA with an optimized P_2O_5 content. Thus, the in-situ polymerization of PBA in the presence of dispersed VGCNF was carried out with different PBA:VGCNF ratios as shown in Scheme 1 and Table 2. The initial color of the reaction mixture was black because of the VGCNF dispersion. As the reaction continued at the polymerization temperature, the color of the reaction mixture changed from black to deep purple-brown. As the amount of VGCNF increased in the polymerization mixture (dopes), the cutoff for the reaction time was generally longer than 48 h because the viscosity had reached the point that the dope stuck to the stirring rod, preventing further efficient stirring via shearing the mixture against the vessel walls and thus requiring a longer heating period. In all cases, the dopes eventually stuck to the stirring rod, and this provided a visual signal that high-MW polymers were being synthesized. However, in the cases with lower VGCNF contents (1−5%), the formation of an insoluble gel was observed when the reaction time was longer than 6 h. Thus, the polymerization process was terminated at certain times when, by judging visually, the viscosities of the dopes had reached a desired level. Such empirical assessment appears to be workable as evidenced by the excellent agreement between the weight percentages of carbon numbers from elemental analysis and the theoretical values for all compositions. The results are summarized in Table 2. The FT-IR spectrum of 10 wt % *m*PEK-*g*-VGCNF (Figure 1b) depicts practically all the IR bands shown in that for pure *m*PEK.

Solution Properties. The polymer products containing 1−10 wt % VGCNF were soluble in NMP but more readily soluble in MSA to form clear and homogeneous solutions. After their MSA solutions had been filtered through glass filter, the filtrates were used to measure the intrinsic viscosities (1.00−1.73 dL/g at 30 ± 0.1 °C in MSA; Table 3). *m*PEKs containing VGCNF from 20 to 30 wt % formed a cloudy solution in MSA. The attempts to obtain via similar filtration the solutions that were sufficiently clear for viscosity measurement were not successful. However, their solutions were homogeneous enough to cast good quality films. A tough and smooth film was cast from *m*PEK containing 10 wt % VGCNF in MSA solution at 85 °C under reduced pressure (1 mmHg).

Thermal Properties. The T_g's of *m*PEK-*g*-VGCNF samples were determined by DSC. The DSC scans were run on the powder samples after they had been heated

Table 3. Thermal Properties of *m*PEK-*g*-VGCNF Samples

calcd composition (wt %)		T_g (°C)		TGA			
				in air		in helium	
VGCNF	*m*PEK	DSC	TMA	$T_{d5\%}$ (°C)	char at 650 °C (wt %)	$T_{d5\%}$ (°C)	char at 650 °C (wt %)
100.0	0.0	ND	ND	682.7	98.2	696.8	96.7
31.9	68.1	157.6	164.2	448.2	31.7	409.0	68.6
21.5	78.5	151.8	153.9	408.6	20.5	388.6	63.1
10.8	89.2	143.7	145.4	430.5	11.4	406.8	55.3
5.4	94.6	143.7	141.2	492.4	5.6	479.9	61.9
2.2	97.8	141.0	138.5	485.7	2.0	478.0	53.7
1.1	98.9	142.5	141.5	477.5	1.2	463.1	54.6
0.0	100.0	136.6	137.1	414.2	0.8	365.6	48.3

Table 4. Calculation of Total Number of Grafting Sites and Degree of Polymerization (DP) for *m*PEK-*g*-VGCNF Samples

sample	wt % (CNF/*m*PEK)[a]	mol CNF[b]	mol *m*PEK[b]	mol grafting sites[c]	*m*PEK DP/chain[d]	*m*PEK MW/chain[e]
30/70	31.7/68.3	2.642	0.348	0.0793	4	862
20/80	20.5/79.5	1.708	0.405	0.0513	8	1551
10/90	11.4/88.6	0.950	0.452	0.0285	16	3109
5/95	5.6/94.4	0.467	0.481	0.0140	34	6743
2/98	2.0/98.0	0.167	0.499	0.0050	100	19601
1/99	1.1/98.8	0.100	0.504	0.0030	168	32935

[a] TGA (air) data. [b] For a 100 g sample, mol (CNF) = wt (CNF)/12.00 and mol(*m*PEK) = wt (*m*PEK)/196.20 (FW $C_{13}H_8O_2$). [c] Total number of grafting sites (mol): mol(CNF) × 0.03 based on the assumption that there are 3 arylcarbonylation sites for every 100 carbons of the VGCNF. [d] Degree of polymerization (DP)/chain = mol(grafting sites)/mol(CNF). [e] MW (*m*PEK) = DP × 196.20 (FW $C_{13}H_8O_2$).

to 200 °C in the DSC chamber and allowed to cool to ambient temperature under nitrogen purge. The T_g was taken as the midpoint of the maximum baseline shift from the second run. As shown in Figure 3 and summarized in Table 2, pristine *m*PEK displayed a T_g at 136.6 °C.[32] As the amount of VGCNF increased, the T_g's of the blends were gradually increased to 157.6 °C for 30 wt % *m*PEK-*g*-VGCNF. This is consistent[33] with the rationale that the attachment of flexible *m*PEK chains to the rigid VGCNF surface imposes constraints over their mobility, resulting in as much as a 21 °C increase in the glass-transition temperature.

To corroborate the DSC results shown in Figure 4 and Table 3, thermomechanical analysis (TMA) was also conducted to obtain more reliable T_g values of samples. As shown in Figure 5 and Table 3, the T_g values from samples with VGCNF content ranging from 1 to 20 wt % were similar to those from DSC experiments. There is a discrepancy of about 6 °C between DSC and TMA data from the sample with 30 wt % VGCNF. This could be because of greater uncertainty, since the baseline shift in the DSC curve was not as clear for this sample as for the others. It should be pointed out that in all samples only a single T_g was detected by both DSC and TMA, strongly implying that all the samples must be constituted with only the grafted product, *m*PEK-*g*-VGCNF. However, this is in contrast to the case that similar grafting reaction of rigid-rod poly(*p*-phenylenebenzobisthiazole) with randomly distributed 2,6-dimethylphenoxy pendants (as grafting sites) with the same AB monomer (3-phenoxybenzoic acid) resulted in a significant amount of unattached, low-MW *m*PEK homopolymers ([η] = 0.1 dL/g) isolated via extraction with methylene chloride.[34]

The TGA experiments on the powder sample of pure VGCNF indicated that the temperatures at which 5% weight loss ($T_{d5\%}$) occurred were at 683 °C in air and 697 °C in helium (Figure 5). All *m*PEK's with and without VGCNF displayed $T_{d5\%}$ in the range 408−448 °C in air and 365−409 °C in helium, respectively. The char percentage at 650 °C in air after *m*PEK had been thermooxidatively stripped off was used to determine the amount of residual VGCNF. The results were in excellent agreement between the theoretical and experimental values for the *m*PEK/VGCNF compositions (Table 3). The results also lend support to our belief that the VGCNF remained more or less structurally intact during the in-situ polymerization and workup.

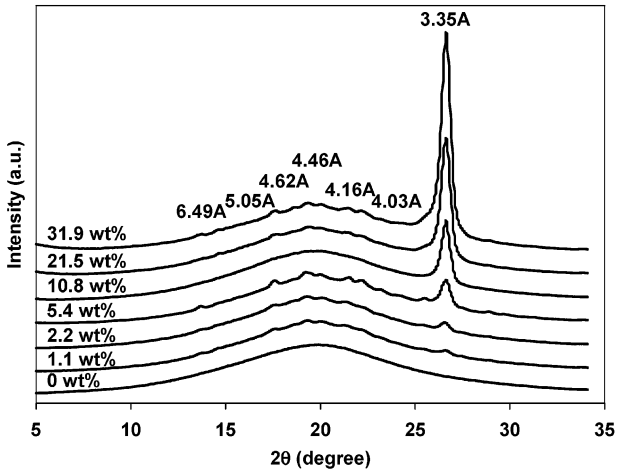

Figure 6. Wide-angle X-ray diffraction patterns of *m*PEK-*g*-VGCNF samples.

Degree of Polymerization (DP) for the *m*PEK Grafts. On the basis of the experimental results in our previous study, we have proposed that, with appropriate ether−arylcarboxylic acid, functionalization of VGCNF via Friedel−Crafts acylation reaction in PPA:P_2O_5 (w/w 4:1) medium could result in arylcarbonylation of three carbons in every 100 carbon sites.[20] Furthermore, the arylcarbonylation reaction is most likely to occur at the sp^2 C−H defect sites. On the basis of this assumption, we have determined the upper-limit values for the DP and molecular weight of each VGCNF-bound *m*PEK, ranging from a DP of 4 with the corresponding MW of 862 Da to a DP of 168 and MW of 32 935 Da. Our computation algorithm and results are shown in Table 4.

Wide-Angle X-ray Diffraction (WAXD). To correlate with the thermal analysis data, all samples were also examined with the wide-angle X-ray diffraction technique to shed further light on the relative amounts

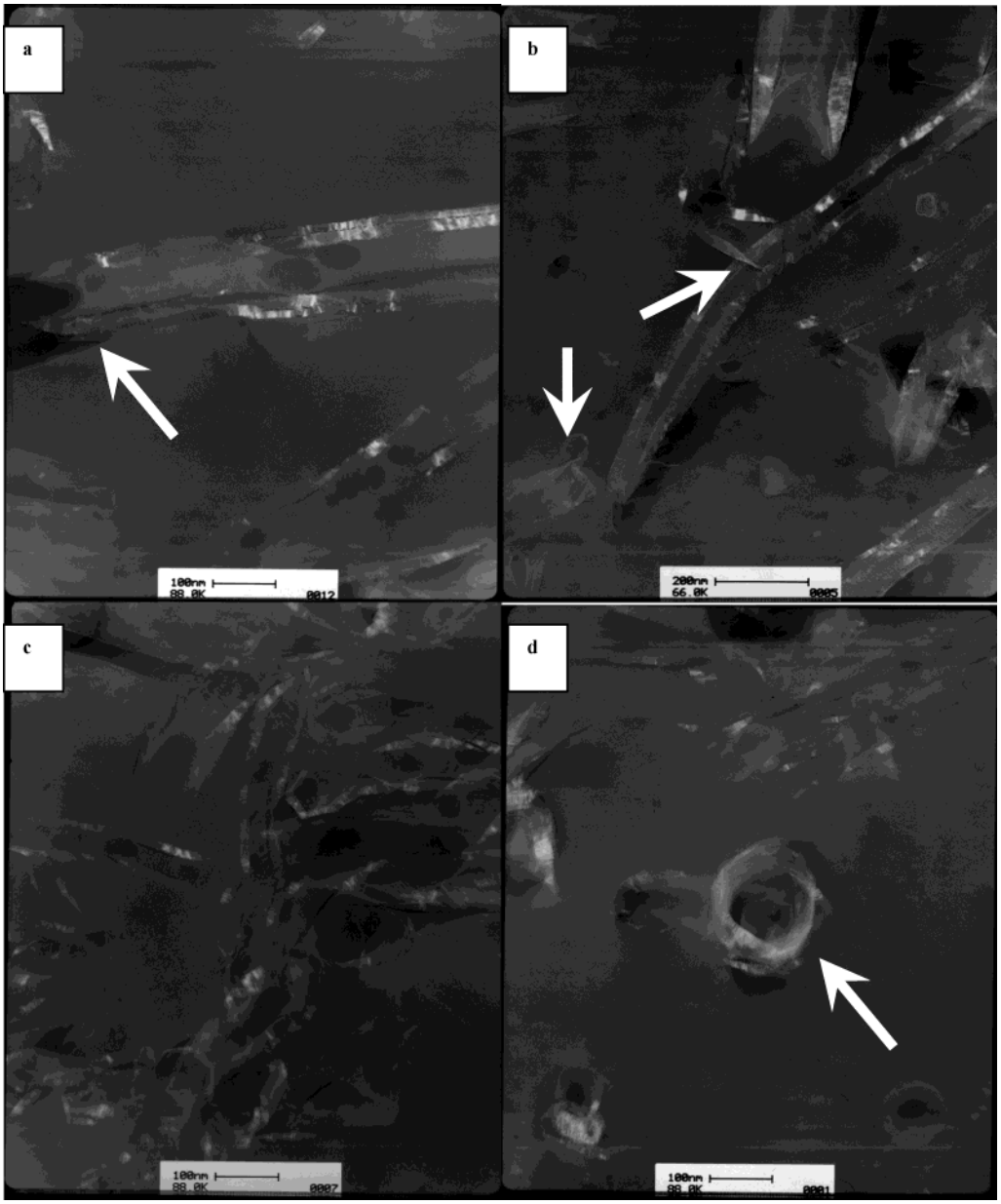

Figure 7. TEM images obtained from powder sample of 30 wt % *m*PEK-*g*-VGCNF with the following magnification: (a) ×88K, (b) ×66K, (c) ×88K, and (d) top view, ×88K. The scale bar is 100 nm.

of VGCNF in the samples as well as the degree of ordering. As depicted in Figure 6, the homopolymer, *m*PEK, is expectedly amorphous as indicated by its featureless WAXD pattern. Also, a characteristic peak that has appeared at 3.35 Å for all VGCNF-containing samples is attributed to the "wall-to-wall" *d* spacing of VGCNF. As expected, its intensity increases proportionally with the amount of VGCNF present in the samples. Finally, it is important to point out that whereas all the VGCNF-containing samples display six weak yet discernible peaks (6.48, 5.05, 4.62, 4.46, 4.16, 4.03 Å), the *m*PEK does not. The latter observation implicates that VGCNF can serve as a template for the local ordering of the covalently attached *m*PEK.

Transmission Electron Microscopy (TEM) Study. The TEM images of a selected sample (*m*PEK with 30 wt % VGCNF; powder) showed that the VGCNF with *m*PEK grafts has still maintained the diameter of 100−200 nm and wall thickness of 20−40 nm, suggesting the relative stability of its nanostructural framework under the polymerization and workup conditions (Figure 7a−d). As clearly observed by TEM, VGCNF is indeed a hollow tube with diameter of 100−200 nm and wall thickness of 20−40 nm (Figure 7a). Also observed are some tubes that have open ends. In addition, some fibril-like features were seemingly attached to the VGCNF, indicative of some covalent bonding. An isotropic distribution of VGCNF also observed, most likely as a result of the uniaxial shear force (mechanical stirring) applied during polymerization in a very viscous medium (Figure 7c). As shown in Figure 7d, the "bird's view" image shows that a tube end of VGCNF was not as sharply defined as that of pristine VGCNF, indicating that *m*PEK was also attached onto at the open end of VGCNF.

Scanning Electron Microscopy (SEM). The SEM image of pristine VGCNF shows that the tube surfaces are clean, and the average diameter is in the range 100−200 nm (Figure 8a). Some tubes have smooth surfaces, and some are bamboo-shaped. The surface of 20 wt % *m*PEK-*g*-VGCNF is rough and fat (Figure 8b) with a diameter of approximately 400 nm. The fuzzy surface of the fat tube appeared to be heavily coated

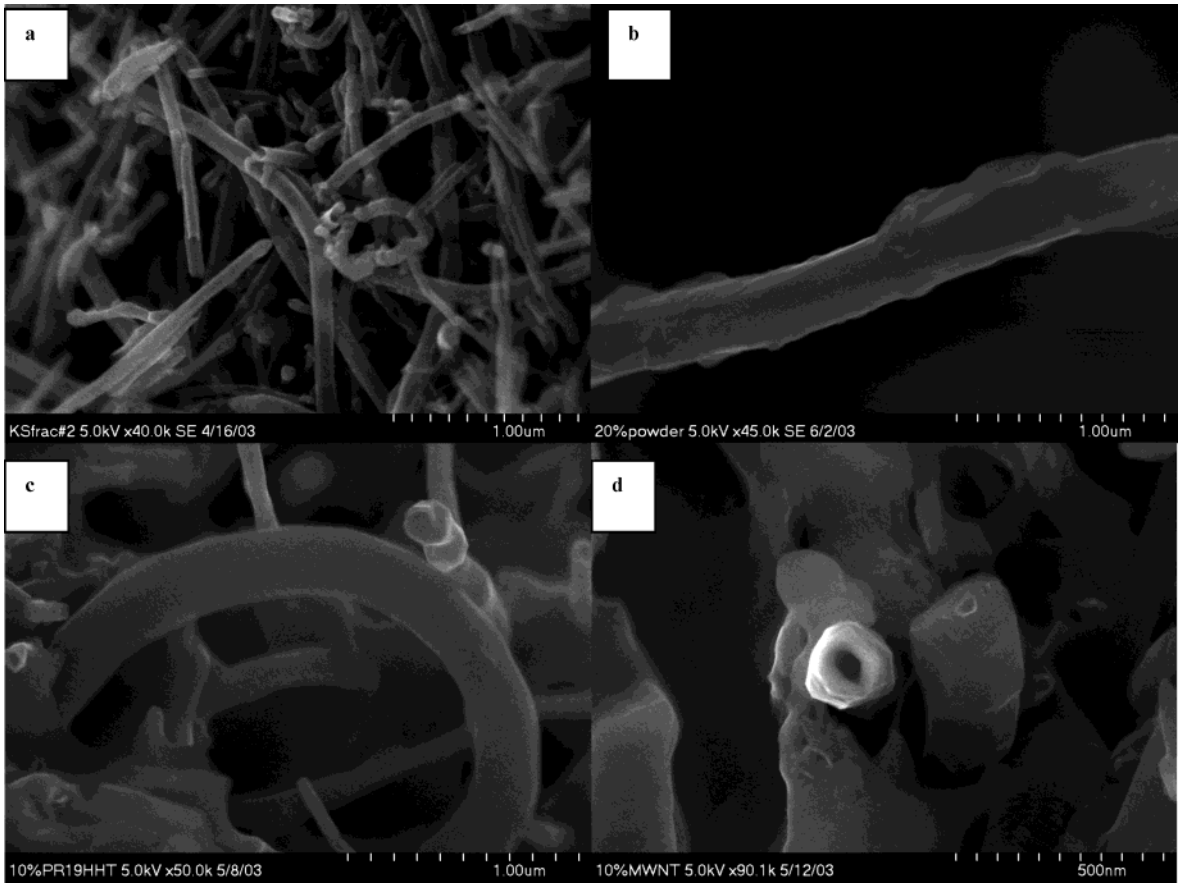

Figure 8. SEM images: (a) as-received VGCNF (×40K); (b) 20 wt % *m*PEK-*g*-VGCNF before heat treatment at 230 °C (×45K); (c) 10 wt % *m*PEK-*g*-VGCNF VGCNF after heat treatment at 230 °C (×50K); (d) 10 wt % VGCNF after heat treatment at 230 °C (× 90K).

with *m*PEK, thus strongly indicative of polymer graft on the surface of VGCNF. The internal diameter of 20 wt % *m*PEK-*g*-VGCNF ranged from 150 to 400 nm, and it could be doubtlessly distinguished from unmodified VGCNF (Figure 8a). Thus, the thickness of the *m*PEK wall for 20 wt % *m*PEK-*g*-VGCNF is approximately 25−150 nm. When the 10 wt % *m*PEK-*g*-VGCNF was compression-molded at 230 °C, the molten *m*PEK spread and coated the surfaces of tubes, transforming them into fat tubes with much smoother surfaces (Figure 8c). The SEM image viewed at the end of a vertical VGCNF clearly showed that the tube tips were almost sealed close by the molten *m*PEK (Figure 8d). Thus, on the basis of the combined results from TEM and SEM studies, it could be reaffirmed that the Friedel−Crafts acylataion in PPA was effective in covalently connecting *m*PEK onto the walls and open ends of VGCNF.

Conductivity Measurement. The 10 wt % *m*PEK-*g*-VGCNF was dissolved in MSA and cast film on the quartz-casting dish at 85 °C in vacuo. The dc electrical conductivity of the resulting film measured by the standard four-probe method was 0.25 and 0.30 S/cm for the bottom of film (quartz side) and top of film (air side), respectively. It is more than 12 orders of magnitude greater than the conductivity ($\sim 1 \times 10^{-14}$ S/cm) of the composite fiber derived from rigid-rod poly(*p*-phenylene-benzobisoxazole) and SWNT (PBO/SWNT; w/w 90/10), prepared via in-situ polymerization in poly(phosphoric acid).[10] A plausible explanation for this discrepancy is that SWNT may have broken down under the polymerization conditions.

Conclusion

While there are limited examples in the literature showing the possibility of in-situ polyadditon of styrenic[12] or acrylic[19] monomers via free-radical processes that effectively grafted the respective poly(olefin) to either MWNT or SWNT, we believe our work is the first case showing the feasibility of grafting an aromatic poly(ether−ketone) to the attendant VGCNF via in-situ polycondensation of the corresponding AB monomer. Furthermore, our method has provided several points of fundamental significance. First, it indicates that PPA is quite effective in dispersing VGCNF because of its acidic and viscous character. We believe that the former property promotes deaggregation of VGCNF, and the latter impedes the rebundling of VGCNF. Second, with the exception of the work by Prato et al., who reported the first application of an electrophilic addition reaction to chloroalkylate the sidewall of SWNT, followed by hydrolysis and O-acylation (esterification) of the SWNT-bound hydroxyl groups,[35] the general nature of almost all chemical reactions utilized in CNT covalent functionalization to date[36] are compatible with the electron-deficient character of the carbon nanotubes. Our work has shown that the defective sp^2 C−H sites of VGCNF are susceptible to electrophilic reactions such as Friedel−Crafts acylation. Last but not least, while we are not aware of any grafting of VGCNF via polyaddition processes, we have, nevertheless, provided a grafting route to generate VGCNF nanocomposites[37] with the potential applicability to both aliphatic and wholly aromatic (high-temperature) polymer matrices.

Acknowledgment. We thank Marlene Houtz (TGA) and Gary Price (WAXD and SEM) of University of Dayton Research Institute, Heather Dowty, and Max Alexander (dc conductivity) of the U.S. Air Force Research Laboratory for the respective characterization data, Dr. Robert Wheeler of UES, Inc., for assistance in TEM imaging, and Prof. Wansoo Huh of Soongsil University for helpful discussions. This work was supported by U.S. Air Force Office of Scientific Research and by a research grant (No. R05-2004-000-10215-0) from Korean Science and Engineering Foundation.

References and Notes

(1) Carneiro, O. S.; Covas, J. A.; Bernardo, C. A.; Caldeira, G.; Hattum, F. W. J. V.; Ting, J. M.; Alig, R. L.; Lake, M. L. *Compos. Sci. Technol.* **1998**, *58*, 401−407.
(2) Singh, C.; Quested, T.; Boothroyd, C. B.; Thomas, P.; Kinloch, I. A.; Abou-Kandil, A. I.; Windle, A. H. *J. Phys. Chem. B* **2002**, *106*, 10915−10922.
(3) Maruyama, B.; Alam, K. *SAMPE J.* **2002**, *38*, 59−70.
(4) (a) Sandler, J.; Shaffer, M. S. P.; Lam, Y.-M.; Windle, A. H.; Werner, P.; Altstadt, V.; Nastalczyk, J.; Broza, G.; Schulte, K.; Keun, C.-A. *Mater. Res. Soc. Symp. Proc.* **2002**, *706*, 105−110. (b) Lozano, K.; Barrera, E. V. *J. Appl. Polym. Sci.* **2001**, *79*, 125−133. (c) Lozano, K.; Bonilla-Rios, J.; Barrera, E. V. *J. Appl. Polym. Sci.* **2001**, *80*, 1162−1172. (d) Ma, H.; Zeng, J.; Realff, M. L.; Kumar, S.; Schiraldi, D. A. *Polym. Mater. Sci. Eng.* **2002**, *86*, 411−412.
(5) (a) Richard, P.; Prasse, T.; Cavaille, J. Y.; Chazeau, L.; Gauthier, C.; Duchet, J. *Mater. Sci. Eng., A* **2003**, *A352*, 344−348. (b) Pittman, C. U., Jr.; Wang, L.; Ni, H.; Li, G. Z. *Abstracts of Papers, 225th ACS National Meeting, New Orleans, LA, March 23−27, 2003;* MTLS-008.
(6) (a) Frogley, M. D.; Ravich, D.; Wagner, H. D. *Compos. Sci. Technol.* **2003**, *63*, 1647−1654. (b) Jacobsen, R. L.; Glasgow, D. G. *Proc. Am. Soc. Compos., Tech. Conf.* **1999**, *14th*, 987−994.
(7) Andrews, R.; Jacques, D.; Qian, D.; Rantell, T. *Acc. Chem. Res.* **2002**, *35*, 1008−1017.
(8) Wang, C. S.; Alexander, M. D. U.S. Patent 6,680,016, Jan 20, 2004.
(9) An attempt to disperse similar vapor-grown carbon fibers via in-situ polymerization of an aromatic, phosphine oxide-containing diamine and oxydiphthalic dianhydride was reported: Watson, K. A.; Smith, J. G., Jr.; Connell, J. W. *Int. SAMPE Tech. Conf.* **2001**, *33*, 1551−1560.
(10) Kumar, S.; Dang, T. D.; Arnold, F. E.; Bhattacharyya, A. R.; Min, B. G.; Zhang, X.; Vaia, R. A.; Park, C.; Adams, W. W.; Hauge, R. H.; Smalley, R. E.; Ramesh, S.; Willis, P. A. *Macromolecules* **2002**, *35*, 9039−9043.
(11) Fan, J.; Wan, M.; Zhu, D.; Chang, B.; Pan, Z.; Xie, S. *J. Appl. Polym. Sci.* **1999**, *74*, 2605−2610.
(12) Tang, B. Z.; Xu, H. *Macromolecules* **1999**, *32*, 2569−2576.
(13) Cochet, M.; Maser, W. K.; Benito, A. M.; Callejas, M. A.; Martínez, M. T.; Benoit, J.-M.; Schreiber, J.; Chauvet, O. *Chem. Commun.* **2001**, *16*, 1450−1451.
(14) Xia, H.; Wang, Q.; Qiu, G. *Chem. Mater.* **2003**, *15*, 3879−3886.
(15) (a) Park, C.; Wise, K.; Ounaies, Z.; Pawlowski, K.; Working, D.; Lowther, S.; Lillehei, P.; Siochi, E.; Harrison, J. *Polym. Mater. Sci. Eng.* **2004**, *90*, 56−57. (b) Park, C.; Ounaies, Z.; Watson, K. A.; Crooks, R. E., Jr.; J. S.; Lowther, S. E.; Connell, J. W.; Siochi, E. J.; Harrison, J. S.; St. Clair, T. L. *Chem. Phys. Lett.* **2002**, *364*, 303−308.
(16) Shaffer, M. S. P.; Koziol, K. *Chem. Commun.* **2002**, 2074−2075.
(17) Smith, J. G., Jr.; Connell, J. W.; Delozier, D. M.; Lillehei, P. T.; Watson, K. A.; Lin, Y.; Zhou, B.; Sun, Y.-P. *Polymer* **2004**, *45*, 825−836.
(18) (a) Hill, D. E.; Lin, Y.; Rao, A. M.; Allard, L. F.; Sun, Y.-P. *Macromolecules* **2002**, *35*, 9466−9471. (b) Sun, Y.-P.; Fu, K.; Lin, Y.; Huang, W. *Acc. Chem. Res.* **2002**, *35*, 1096−1104.
(19) (a) Kong, H.; Gao, C.; Yan, D. *J. Am. Chem. Soc.* **2004**, *126*, 412−413. (b) Baskaran, D.; Mays, J. W.; Bratcher, M. S. *Angew. Chem., Int. Ed.* **2004**, *43*, 2138−2142.
(20) Baek, J.-B.; Lyons, C.; Tan, L.-S. *J. Mater. Chem.* **2004**, *14*, 2052−2056.
(21) http://www.apsci.com.
(22) (a) Kim, C.; Yang, K. S. *Appl. Phys. Lett.* **2003**, *83*, 1216−1218. (b) Wang, Y.; Serrano, S.; Santiago-Aviles, J. J. *J. Mater. Sci., Lett.* **2002**, *21*, 1055−1057. (c) Wang, Y.; Serrano, S.; Santiago-Aviles, J. J. *Synth. Met.* **2003**, *138*, 423−427.
(23) For a TEM picture of "Pyrograf" nanofibers showing a bamboo-like structure, see: Richard, P.; Prasse, T.; Cavaille, J. Y.; Chazeau, L.; Gauthier, C.; Duchet, J. *Mater. Sci. Eng., A* **2003**, *A352*, 344−348.
(24) Schaefer, D. W.; Brown, J. M.; Anderson, D. P.; Zhao, J.; Chokalingam, K.; Tomlin, D.; Ilavsky, J. *J. Appl. Crystallogr.* **2003**, *36*, 553−557.
(25) (a) Alexander, M. D., Jr.; Bentley, H.; Wang, C.-S. *Polym. Prepr. (Am. Chem. Soc., Div. Polym. Chem.)* **2003**, *44*, 294−295. (b) Stuckey, J. A.; Alexander, M. D., Jr.; Black, B. M.; Henes, J. D. *Polym. Prepr. (Am. Chem. Soc., Div. Polym. Chem.)* **2003**, *44*, 141−142.
(26) Endo, M.; Nishimura, K.; Kim, Y. A.; Hakamada, K.; Matushita, T.; Dresselhaus, M. S.; Dresselhaus, G. *J. Mater. Res.* **1999**, *14*, 4474−4477.
(27) (a) Bahr, J. L.; Yang, J.; Kosynkin, D. V.; Bronikowski, M. J.; Smalley, R. E.; Tour, J. M. *J. Am. Chem. Soc.* **2001**, *123*, 6536−6542. (b) Bahr, J. L.; Tour, J. M. *J. Mater. Chem.* **2002**, *12*, 1952−1958. (c) Bahr, J. L.; Tour, J. M. *Chem. Mater.* **2001**, *13*, 3823−3824.
(28) Bandow, S.; Asaka, S.; Saito, Y.; Rao, A. M.; Grigorian, L.; Richter, E.; Eklund, P. C. *Phys. Rev. Lett.* **1998**, *80*, 3779−3782.
(29) Holzinger, M.; Abraham, J.; Whelan, P.; Graupner, R.; Ley, L.; Hennrich, F.; Kappes, M.; Hirsch, A. *J. Am. Chem. Soc.* **2003**, *125*, 8566−8580.
(30) Smith, J. G., Jr.; Connell, J. W.; Delozier, D. M.; Lillehei, P. T.; Watson, K. A.; Lin, Y.; Zhou, B.; Sun, Y.-P. *Polymer* **2004**, *45*, 825−836.
(31) Dresselhaus, M. S.; Dresselhaus, G.; Jorio, A.; Filho, A. G. S.; Pimenta, M. A.; Saito, R. *Acc. Chem. Res.* **2002**, *35*, 1070−1078.
(32) Baek, J.-B.; Tan, L.-S. *Polymer* **2003**, *44*, 4135−4147.
(33) On the contrary, the presence of 0.1−0.2 wt % of a similar VGCNF in an aromatic polyimide was reported to have decreased the T_g of the base polymer by 10−12 °C; see ref 9.
(34) Dotrong, M.; Dotrong, M. H.; Evers, R. C. *Polymer* **1993**, *34*, 726−730.
(35) Tagmatarchis, N.; Georgakilas, V.; Prato, M.; Shinohara, H. *Chem Commun. (Cambridge)* **2002**, 2010−2011.
(36) (a) Bahr, J. L.; Tour, J. M. *J. Mater. Chem.* **2002**, *12*, 1952−1958. (b) Hirsch, A. *Angew. Chem., Int. Ed.* **2002**, *41*, 1853−1859.
(37) In principle, the products obtained from the foregoing in-situ polymerization process should be *m*PEK-*g*-VGCNF. Although we have not seen any evidence to indicate otherwise, it is, however, still quite possible to contain some *m*PEK homopolymer in the products that was below the detection limits.

MA048964O